Journal of Molecular Catalysis A: Chemical 387 (2014) 112–122

Contents lists available at ScienceDirect

Journal of Molecular Catalysis A: Chemical

journal homepage: www.elsevier.com/locate/molcata

Ligand characteristics and *in situ* generation of Pd active species towards C—C coupling using series of 2-(1H-imidazol-2-yl)phenols

Abiodun O. Eseola[a,b,*], Oluwatimilehin Akogun[a], Helmar Görls[b], Olubunmi Atolani[a], Gabriel A. Kolawole[a,c], Winfried Plass[b]

[a] Department of Chemical Sciences, Redeemer's University, Redemption Camp, Ogun State, Nigeria
[b] Institut für Anorganische und Analytische Chemie, Friedrich-Schiller-Universität Jena, Humboldtstr. 8, D-07743 Jena, Germany
[c] Research Fellow, University of Zululand, Private Mail Bag X1001, Kwadlangezwa 3886, South Africa

ARTICLE INFO

Article history:
Received 5 December 2013
Received in revised form 9 February 2014
Accepted 27 February 2014
Available online 7 March 2014

Keywords:
Homogeneous catalysis
Carbon–carbon cross-coupling
In situ catalyst formation
Suzuki–Miyaura
Structure–property correlation

ABSTRACT

Series of systematically varied 2-(1H-imidazol-2-yl)phenol ligand frameworks, which were synthesized and properly characterized, have been used to investigate favourable ligand characteristics towards *in situ* formation of active palladium species in Suzuki–Miyaura coupling. Structures of 2-(4,5-diethyl-1H-imidazol-2-yl)-4-nitrophenol (***p*-N∼de**) and 4-(tert-butyl)-2-(4,5-diphenyl-1H-imidazol-2-yl)phenol (***p*-*t*Bu∼dp**) as well as the palladium complex of 2-(4,5-diethyl-1H-imidazol-2-yl)phenol (**Pd.de$_2$**) were confirmed. Structural analyses show that *para*-nitro-substituted phenol moieties bear poor oxo-donor atom while the reverse was observed for *para*-*t*Bu-substituted analogues. Ligand donor strengths were also determined by pK_a analysis.

Under the same reaction conditions for palladium catalyzed Suzuki–Miyaura coupling in the presence of 'ligand + palladium(II) acetate' catalyst system, results show that electronic properties of the ligands are more important than the variation in steric properties. In particular, ligands with strong bidentate chelate coordination potentials acted as poisons while those with monodentate coordination potential proved to be very beneficial towards *in situ* generation of superior active species. Furthermore, correlation between donor strength pK_a data and the trends in catalytic efficiencies as a consequence of ligand presence was studied. Therefore, it was concluded that ligands with strong chelation tendencies adversely impacted *in situ* palladium catalyst generation efficiency and that there appears to be moderate steric requirement from ligands for optimal catalyst efficiency.

1. Introduction

Palladium catalyzed cross-coupling reactions are inevitable organometallic tools for synthetic organic manipulations in the present day molecular sciences [1–7]. Fields in molecular sciences such as drug design, natural product total synthesis, supramolecular architectural ligand designs and structure–property relationship investigations, have come to recognize the various Pd-catalyzed C—C bond forming reactions as a seamless route to otherwise impossible organic synthetic destinations [8–10]. Recognition of the importance and ease with which palladium species accomplish C—C coupling events lead to the recent award of Nobel Prize for Chemistry (2010) in honour of the pioneering works of Suzuki, Heck and Negishi [11–17]. Suzuki–Miyaura catalysis, which is the cross-coupling of an aryl halide with boron-containing reagents in the presence of palladium species and a base additive, is prominently employed amongst other popular Pd-catalyzed C—C coupling methods like Heck, Sonogashira, Stille, Negishi, Kumada, Hiyama, *etc.* [18–24]. Even some notably efficient catalytic palladium compounds have already been commercialized; *e.g.* PEPPSI™ [25].

Nearly all reported forms of palladium materials have been implicated as active catalytic species towards C—C cross-coupling [26–28]. Hence, the true homogeneous/heterogeneous nature of the active species has continued to be a subject of discussion [27–30]. For instance, some recent contribution reported that unprecedented homogeneous catalyst performance was encountered for soluble Pd(0) species bearing monodentate ligands with sterically bulky groups (*i.e.* Buchwald ligands, *etc.*) [5,10,31,32] while other views believe that high activities in Pd-catalyzed C—C

* Corresponding author at: Department of Chemical Sciences, Redeemer's University, Redemption Camp, Ogun State, Nigeria. Tel.: +234 07062192104.
E-mail addresses: bioduneseola@hotmail.com, bioduneseola@run.edu.ng (A.O. Eseola).

http://dx.doi.org/10.1016/j.molcata.2014.02.032
1381-1169/

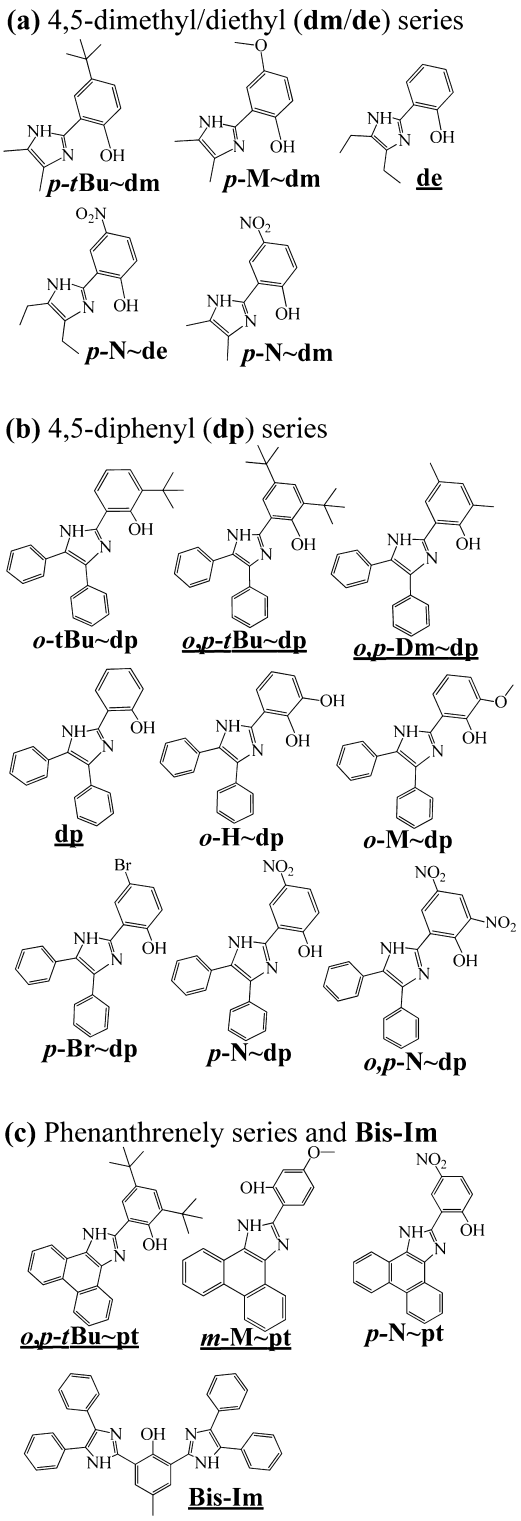

Scheme 1. (a)–(c) Ligand frameworks employed in this study ([a]the underlined were synthesized according to recent reports [53–55]).

cross-coupling reactions should be attributed to ligandless palladium species [29,33,34]. Consequently, improved understanding of ligand effects is necessary and is achievable by studying complexes derived from series of rationally varied ligand framework. However, there seem to be more focus on optimizing catalyst properties of few materials.

Substantial depth of study on ligand effects cannot be accomplishable with heterogeneously supported catalysts [33,35–37] mainly because, among other set-becks, there are relatively more limitations for surface catalyst characterization unlike the possibility of detailed electronic/structural characterization for discrete drop-in homogeneous catalyst precursor systems [38–41]. In homogeneous catalytic investigations, applying properly characterized metal complex series derived from their corresponding series of rationally varied ligand frameworks is an important method used to pursue better understanding of the active site formation and/or compositions as well as to study the relevant underlying mechanisms [10,42–47]. However, such systematic investigation involving suitable number of palladium species derived from ligands of well studied and deliberately varied hemilability trends is scarce.

In situ catalyst formation method is considered to be attractive because it obliterates necessity for the additional tasks of prior syntheses of the corresponding palladium complexes and it also enables the flexibility of selecting ligand types to accompany available palladium salts depending on a specific cross-coupling catalysis requirement [43–45,48,49]. However, investigating dependence of catalysis outcomes on ligand presence and ligand types for *in situ* methods is scarce unlike studies with preformed free or supported palladium complexes. Furthermore, little attention is usually paid to the fact that the substrates, which are usually present in large excess relative to catalytic amounts of added organic ligands, may possess strongly coordinating heteroatoms and thus influence active site generation. It is worthy of note that, while preformed palladium complexes would often require some form of complex disassembly under elevated temperatures in order to provide vacant coordination sites, employing mixture of palladium salt and ligand as the catalytic system may assemble up to similar active state configurations. Therefore, it was considered reasonable to study effect of ligand presence and the trends in ligand characters that would favour generation of superior active sites while maintaining all other factors constant.

In our recent reports, experimental and DFT studies showed that a series of 2-(1H-imidazol/oxazol-2-yl)phenol and 2-(1H-imidazol/oxazol-2-yl)pyridine ligand families are hemilabile and that donor intensities of the imidazole/oxazole arm of the bidentate ligands could vary from very poorly donating to fairly strongly donating. The difference depends on the variation of substituent environment around the 2-(1H-imidazol-2-yl)pyridine or 2-(1H-imidazol-2-yl)phenol basic skeletons as well as on azole ring heteroatom (*i.e.* whether the imidazole ring is replaced by oxazole ring) [50–56]. Motivated by the potentials of these previously studied ligands to shed some light on effects of ligand presence during *in situ* catalyst formation towards Pd-catalyzed C—C coupling reactions, we herein present results for ligand syntheses and the corresponding catalytic studies on their Pd-ligand coordination species, which are generated *in situ* under similar catalytic reaction condition for a series of bidentate 2-(1H-imidazol-2-yl)phenol library. The ligands employed in this study are rationally varied in terms of structural and electronic diversity (Scheme 1(a)–(c)). Synthesis and catalytic behaviour of the palladium complex of ligand **de** is also presented for comparison.

2. Experimental

2.1. General considerations

All starting materials were obtained commercially as reagent grades and used without further purification. Preparation and characterization of ligands **de**, **dp**, **m-M~pt**, ***o,p*-Dm~dp**, ***o,p*-*t*Bu~dp**, **o,p-*t*Bu~pt** and **Bis-Im** were according to published procedures [51,53,54]. The synthesized organic compounds were either purified on silica gel column or re-crystallized to exclude impurities.

Elemental analyses were performed on Leco CHNS-932 or El Vario III elemental analyzers. ^{1}H and ^{13}C NMR spectra were recorded on a Bruker ARX 200 or 400 MHz instrument using deuterated solvents and TMS as internal standard. IR spectra were recorded on a Nicolet 6700 or Shimadzu 8740 FT-IR spectrometer as KBr discs and measurements were done in the range of 4000–400 cm^{-1}. Single crystal X-ray data collections were carried out on a Nonius Kappa CCD diffractometer at 133(2) K using graphite monochromated Mo-Kα radiation (k = 0.71073 Å). Cell parameters were obtained by global refinement of the positions for all collected reflections. The structures were solved by direct methods and refined by full-matrix least-squares on F2. All non-hydrogen atoms were refined anisotropically. The imidazole ring protons, the phenolic protons as well as other protons were actually picked on the difference maps during structure refinement. Structure solutions and refinements were performed using the SHELX-97 package [57].

2.2. Preparation of the ligands

2.2.1. 4-Tert-butyl-2-(4,5-dimethyl-1H-imidazol-2-yl)phenol (***p*-*t*Bu∼dm**)

A mixture of 5-tert-butyl-2-hydroxybenzaldehyde (1.70 g, 9.54 mmol), butane-2,3-dione (0.82 g, 9.54 mmol) and ammonium acetate (≈10 g, 129.73 mmol) were refluxed in the presence of 1 mL glacial acetic acid for 1.5 h. The resulting reaction solution was cooled, diluted with distilled water (≈30 mL), neutralized by concentrated ammonia solution and the crude product was extracted with dichloromethane, concentrated and purified on silica gel column using ethyl acetate/n-hexane (1:4) as eluent to obtain ***p*-*t*Bu∼dm** (0.41 g, 18%). Mp. 258–259 °C. Selected IR peaks (KBr, cm^{-1}): ν 3244s (imidazole proton), 2958s (*t*-Bu and methyl), 2922 m (*t*-Bu and methyl), 1618s (C=C or C=N), 1599s (C=C or C=N). ^{1}H NMR (400 MHz, TMS, $CDCl_3$); δ_{ppm} 7.28 (d, J = 2.0 Hz, 1H, phenol ring); 7.24 (dd, J = 2.4, 8.8 Hz, 1H, phenol ring); 6.97 (d, J = 8.8 Hz, 1H, phenol ring); 2.23 (s, 6H); 1.32 (s, 9H, *t*-Bu). ^{13}C NMR (100 MHz, $CDCl_3$): 154.91, 144.11, 141.19, 126.94, 118.87, 117.06, 112.17, 34.09, 31.57. MS (EI) m/z 244 (M^+, 70%): 244, 229, 214, 199, 100. Anal. Calc. For $C_{15}H_{20}N_2O$: C, 73.74; H, 8.25; N, 11.47%. Found: C, 73.83; H, 8.21; N, 11.31%.

2.2.2. 4-Methoxy-2-(4,5-dimethyl-1H-imidazol-2-yl)phenol (***p*-M∼dm**)

2-Hydroxy-5-methoxybenzaldehyde, (0.75 g, 4.93 mmol), butane-2,3-dione (0.43 g, 4.99 mmol) and ammonium acetate (≈10 g, 129.73 mmol) were reacted and purified in similar manner as for preparation of ***o*-*t*Bu∼dm** above using ethyl acetate/n-hexane (1:1) as eluent. Traces of acetic acid could be observed in the ^{1}H NMR of the eluted compound. Therefore, the eluted product was recrystallyzed from ethanol to obtain ***p*-M∼dm** (0.17 g, 16%). Mp. 243–244 °C. Selected IR peaks (KBr, cm^{-1}): ν 3333vs(vsh, imidazole proton), 2997 m (methyl), 2959s (methyl), 1605s (C=C, C=N), 739s. ^{1}H NMR (400 MHz, TMS, *d6*-DMSO); δ_{ppm} 12.54 (s, 1H); 12.30 (s, 1H), 7.35 (d, J = 2.4 Hz, 1H, phenol ring); 7.12 (d, J = 7.6 Hz, 1H, phenol ring); 6.80 (d, J = 9.2 Hz, 1H, phenol ring); 6.76 (dd, J = 2.8, 8.8 Hz, 1H, phenol ring); 3.73 (s, 3H, methoxy); 2.21 (s, 3H, methyl); 2.11 (s, 3H, methyl). ^{13}C NMR (100 MHz, *d6*-DMSO): 151.74, 150.29, 143.32, 130.24, 121.86, 117.17, 115.45, 113.24, 108.10, 55.54 (methoxy), 11.77, 9.07. MS (EI) m/z 218 (M^+, 98%): 218, 203, 175, 28. Anal. Calc. for $C_{12}H_{14}N_2O_2 \cdot (1/4)$EtOH C, 65.34; H, 6.80; N, 12.19%. Found: C, 65.20; H, 7.12; N, 12.52%.

2.2.3. 2-(4,5-Diethyl-1H-imidazol-2-yl)-4-nitrophenol (***p*-N∼de**)

2-Hydroxy-5-nitrobenzaldehyde (2.00 g, 11.97 mmol), hexane-3,4-dione (1.37 g, 12.00 mmol) and ammonium acetate (18 g, 233.52 mmol) were reacted and purified in similar manner as for preparation of ***o*-*t*Bu∼dm** above to obtain ***p*-N∼de** (1.34 g, 43%). Mp. 188 °C. Selected IR peaks (ATR, cm^{-1}): ν 3372 m (PhOH), 3223 m (imidazole proton), 2973s (ethyl), 2934s (ethyl), 1720s (ethyl acetate C=O), 1647vs (C=O, C=C), 1601vs (C=C, C=N), 1557vs (C=N, C=C), 1144vs, 836vs. ^{1}H NMR (400 MHz, TMS, $CDCl_3$); δ_{ppm} 13.03 (s, 2H, imidazole NH), 8.80 (d, J = 2.6 Hz, 1H, phenol ring), 8.07 (dd, J = 9.2, 2.6 Hz, phenol ring), 6.97 (d, J = 9.2 Hz, 1H, phenol ring), 2.68 (q, J = 7.6 Hz, 4H, ethyl), 1.32–1.22 (m, 6H, ethyl; multiplet due to ethyl acetate superimposition). ^{13}C NMR (101 MHz, $CDCl_3$); δ 171.32, 142.59, 137.47, 125.92, 121.03, 119.02, 112.14, 77.33, 77.01, 76.70, 60.47, 21.08, 18.25, 14.30, 14.19. MS (EI) m/z 261 (M^+, 100%): 261, 246, 231, 215, 200. Anal Calc. for $C_{13}H_{15}N_3O_3 \cdot H_2O$: C, 55.91; H, 6.14; N, 15.05. Found: C, 56.12; H, 6.06; N, 15.41.

2.2.4. 2-(4,5-Dimethyl-1H-imidazol-2-yl)-4-nitrophenol (***p*-N∼dm**)

2-Hydroxy-5-nitrobenzaldehyde (1.67 g, 10.00 mmol), butane-2,3-dione (0.86 g, 10.00 mmol) and ammonium acetate (≈10 g, 129.73 mmol) were reacted and purified in similar manner as for preparation of ***o*-*t*Bu∼dm** above to obtain ***p*-N∼dm** (0.29 g, 12%). Dec. 139 °C. Selected IR peaks (KBr, cm^{-1}): ν 3070w (phenyl protons), 2926 m (methyl), 1653s (C=O, C=C), 1608s (C=C, C=N), 1552s, 752 m. ^{1}H NMR (400 MHz, TMS, *d6*-DMSO); δ_{ppm} 13.83 (s, 2H, NH, phenol OH); 8.79 (d, J = 2.8 Hz, 1H, phenol ring); 8.05 (dd, J = 2.8, 8.8 Hz, 1H, phenol ring); 6.98 (d, J = 9.6 Hz, 1H, phenol ring); 2.19 (s, 6H); trace ethylacetate. ^{13}C NMR (100 MHz, *d6*-DMSO): 164.20, 141.58, 138.00, 126.17, 125.01, 120.47, 118.06, 112.58, 10.01. MS (EI) m/z 233 (M^+, 100%): 233, 203, 187, 159, 28. Anal. Calc. for $C_{12}H_{14}N_2O_2 \cdot (1/10)$EtAcO: C, 56.57; H, 4.91; N, 17.36%. Found: C, 57.11; H, 4.74; N, 17.24% (see supplementary information S1).

2.2.5. 2-Tert-butyl-6-(4,5-diphenyl-1H-imidazol-2-yl)phenol (***o*-*t*Bu∼dp**)

5-Tert-butyl-2-hydroxybenzaldehyde (1.70 g, 9.51 mmol), benzil (2.00 g, 9.51 mmol) and ammonium acetate (14 g, 181.63 mmol) were refluxed in glacial acetic acid (cc. 20 mL) for 2 h. The reaction mixture was cooled, diluted with distilled water (80 mL) and neutralized with aqueous ammonia. The crude product was filtered washed with distilled water and dried. Recrystallization in hot ethanol was carried out to obtain ***o*-*t*Bu∼dp** (1.73 g, 51%). Mp. 204–205 °C. Selected IR peaks (KBr, cm^{-1}): ν 3282s (imidazole proton), 2953s (*t*-Bu), 1600 m (C=C, C=N), 1441s. ^{1}H NMR (200 MHz, TMS, $CDCl_3$); δ_{ppm} 11.37 (s, 1H, NH); 7.60–7.20 (m, 12H, aromatic H); 6.86 (d, J = 7.8 Hz, 1H); 1.47 (s, 9H, *t*-Bu). ^{13}C NMR (50 MHz, $CDCl_3$): 128.86, 127.98, 29.59. MS (EI) m/z 368 (M^+, 100%): 368, 353, 337, 177, 162. Anal. Calc. for $C_{25}H_{24}N_2O$: C, 81.49; H, 6.57; N, 7.60%. Found: C, 81.53; H, 6.51; N, 7.59%.

2.2.6. 3-(4,5-Diphenyl-1H-imidazol-2-yl)benzene-1,2-diol (***o*-H∼dp**)

A mixture of 2,3-dihydroxybenzaldehyde (0.17 g, 1.23 mmol), benzil (0.26 g, 1.23 mmol) and ammonium acetate (1.90 g, 24.65 mmol) were reacted as for the preparation of ***o*-*t*Bu∼dp**, but purified using 1:4 ethyl acetate/n-hexane on silica gel column to afford ***o*-H∼dp** (0.38 g, 94%). Mp. 181–182 °C. Selected IR peaks (KBr, cm^{-1}): ν 3457s(sh, PhOH), 3408s(sh, PhOH), 3217s(sh, imidazole proton), 3055w (phenyl proton), 2984w (acetic acid), 1701vs (acetic acid), 1605 m (C=C, C=N), 1586w, 699s. ^{1}H NMR (400 MHz, TMS, *d6*-DMSO); δ_{ppm} 12.92 (s, 1H, NH); 12.14 (s, 1H, phenolic OH), 8.93 (s, 1H, phenolic OH); 7.50 (m, 8H, 4,5-diphenyl); 7.34 (dd, J = 7.2 Hz, 2H, 4,5-diphenyl); 7.26 (dd, J = 7.2 Hz, 1H); 6.80 (d, J = 8.8 Hz, 1H, phenol ring); 6.74 (dd, J = 2.8 Hz, 8.8 Hz, 1H, phenol ring); 1.91 (acetic acid). ^{13}C NMR (100 MHz, *d6*-DMSO): 172.01(acetic acid), 149.62, 149.51, 145.94, 134.28, 133.75, 130.26, 128.71, 128.48, 128.20, 127.21, 127.01, 126.83, 117.62, 117.15, 112.81, 110.93, 56.01(ethanol), 21.02(acetic acid), 18.54(ethanol). MS (EI) m/z 328 (M^+, 100%): 328, 199, 271, 165. Anal. Calc. for

$C_{21}H_{16}N_2O_2\cdot(3/4)EtOH\cdot(1/4)CH_3COOH$: C, 73.09; H, 5.73; N, 7.41%. Found: C, 73.09; H, 5.56; N, 7.12% (see supporting information).

2.2.7. 2-Methoxy-6-(4,5-diphenyl-1H-imidazol-2-yl)phenol (***o-M*∼*dp***)

2-Hydroxy-3-methoxybenzaldehyde (1.45 g, 9.51 mmol), 1,2-diphenylethanedione (2.00 g, 9.51 mmol) and ammonium acetate (14.76 g, 109.27 mmol) were refluxed overnight at 100 °C in glacial acetic acid (60 mL). The reaction mixture was allowed to cool, diluted with distilled water (≈100 mL) and neutralized with aqueous ammonia. The resulting precipitate was filtered, washed with water and dried. The precipitate was dissolved in chloroform, contacted with water to remove possible residues of ammonium acetate and the organic solution was allowed to stand in order to obtain **o-M**∼**dp** as colourless blocks of crystals (3.02 g, 93%). Mp. 196–197 °C. Selected IR peaks (KBr, cm^{-1}): ν 3281vs(sh) (imidazole proton), 3057 m (phenyl proton), 2937w (methyl), 1602 m (C=C, C=N), 1594 m, 1481s, 1063s. ^{1}H NMR (400 MHz, TMS, $CDCl_3$); δ_{ppm} 7.55 (d, J = 6.8 Hz, 4H, 4,5-diphenyl rings); 7.51 (dd, J = 3.6, 6.0 Hz, 1H); 7.34 (m, 6H); 6.87 (m, 2H); 3.91 (s, 3H). ^{13}C NMR (100 MHz, $CDCl_3$): 148.47, 146.45, 144.99, 131.58, 128.72, 128.06, 127.91, 119.23, 116.87, 112.43, 112.26, 56.20. MS (EI) m/z 342 (M^+, 100%): 342, 324, 312, 299, 165. Anal. Calc. for $C_{22}H_{18}N_2O_2\cdot(2/3)CHCl_3$: C, 64.52; H, 4.46; N, 6.64%. Found: C, 64.37; H, 4.82; N, 6.49%.

2.2.8. 4-Bromo-2-(4,5-diphenyl-1H-imidazol-2-yl)phenol (***p-Br*∼*dp***)

5-Bromo-2-hydroxybenzaldehyde (1.91 g, 9.51 mmol), benzil (2.00 g, 9.51 mmol) and ammonium acetate (12 g, 155.68 mmol) were reacted as for ***o-t*Bu∼dp** in glacial acetic acid (50 mL) to obtain ***p*-Br∼dp** as whites microcrystalline powder (2.89 g, 78%). Mp. 182–183 °C. Selected IR peaks (KBr, cm^{-1}): ν 3408 m (PhOH), 3197s (imidazole proton), 3055 m (phenyl proton), 1605s (C=C, C=N), 1580s, 1074s. ^{1}H NMR (200 MHz, TMS, *d6*-DMSO); δ_{ppm} 13.14 (s, 1H); 13.08 (s, 1H), 8.30 (d, J = 2.4 Hz, 1H, phenol ring); 7.50–7.28 (m, 11H); 7.34 (d, J = 8.6 Hz, 1H, phenol ring). ^{13}C NMR (50 MHz, *d6*-DMSO): 155.82, 144.40, 134.32, 132.34, 128.74, 128.54, 128.39, 127.06, 126.87, 119.06, 114.75, 110.06, 107.38. MS (EI) m/z 390 (M^+, 100%): 390, 283, 193, 165, 141. Anal. Calc. for $C_{21}H_{15}BrN_2O$: C, 64.46; H, 3.86; N, 7.16%. Found: C, 64.85; H, 3.60; N, 7.27%.

2.2.9. 2-(4,5-Diphenyl-1H-imidazol-2-yl)-4-nitrophenol (***p-N*∼*dp***)

2-Hydroxy-5-nitrobenzaldehyde (0.79 g, 4.76 mmol), 1,2-diphenylethanedione (1.00 g, 4.76 mmol) and ammonium acetate (7.30 g, 95.20 mmol) were treated as for ***o-t*Bu∼dp** above to obtain the spectroscopically pure ligand ***p*-N∼dp** as yellow microcrystals in high yield (1.63 g, 95%). Mp. 259–260 °C. Selected IR peaks (KBr, cm^{-1}): ν 3343s (imidazole proton), 3058 m (phenyl ring), 1597s (C=C, C=N), 1581 m, 1339vs. ^{1}H NMR (400 MHz, TMS, *d6*-DMSO); $\delta_{ppm} \approx$ 13.95 (vbr, s, 2H, NH and phenolic OH); 9.15 (s, 1H); 8.18 (d, J = 8.8 Hz, 1H); 7.54 (d, J = 8.0 Hz, 4H, 4,5-diphenyl rings); 7.44 (dd, J = 7.2 Hz, 4H, 4,5-diphenyl rings); 7.38 (dd, J = 7.2 Hz, 2H, 4,5-diphenyl rings); 7.19 (d, J = 9.2 Hz, 1H). ^{13}C NMR (100MHz, *d6*-DMSO): 143.98, 139.66, 131.37, 128.71, 128.01, 127.76, 125.57, 121.30, 111.37. MS (EI) m/z 357 (M^+, 100%): 357, 327, 311, 283, 167. Anal. Calc. for $C_{21}H_{15}N_3O_3\cdot(1/3)H_2O$: C, 69.41; H, 4.35; N, 11.56%. Found: C, 69.54; H, 4.32; N, 11.28%.

2.2.10. 2-(4,5-Diphenyl-1H-imidazol-2-yl)-4,6-dinitrophenol (***o,p-N*∼*dp***)

2-Hydroxy-3,5-dinitrobenzaldehyde (0.35 g, 1.65 mmol), hexane-3,4-dione (0.35 g, 1.65 mmol) and ammonium acetate (2.54 g, 32.95 mmol) were reacted and purified in similar manner as for preparation of ***o-t*Bu∼dm** above to obtain ***o,p*-N∼dp** (0.62 g, 93%). Mp. 341 °C. Selected IR peaks (ATR, cm^{-1}): ν 3141s (imidazole proton), 3086s (phenyl proton), 1641s (C=O, C=C), 1602vs (C=C, C=N), 1561vs, 1268vs, 766vs. ^{1}H NMR (400 MHz, TMS, DMSO); δ_{ppm} 9.11 (d, J = 3.0 Hz, 1H), 8.70 (d, J = 2.9 Hz, 1H), 7.63–7.52 (m, 4H), 7.48 (d, J = 6.7 Hz, 6H). ^{13}C NMR (101 MHz, DMSO) δ 129.00, 129.00, 128.52, 128.30, 128.30, 97.70, 23.98. MS (EI) m/z 402 (M^+, 100%): 402, 356, 309, 281. Anal. Calc. for $C_{21}H_{14}N_4O_5$: C, 62.69; H, 3.51; N, 13.92%. Found: C, 62.79; H, 3.42; N, 13.68%.

2.2.11. 4-Nitro-2-(1H-phenanthro[9,10-d]imidazol-2-yl)phenol (***p-N*∼*pt***)

2-Hydroxy-3,5-dinitrobenzaldehyde (2.00 g, 11.77 mmol), phenanthrene-9,10-dione (2.49 g, 11.77 mmol) and ammonium acetate (18 g, 233.52 mmol) were reacted in similar manner as for preparation of ***o-t*Bu∼dm** above, but the crude product was pure enough to obtain ***p*-N∼pt** (3.68 g, 88%). Mp/Dec. 372 °C. Selected IR peaks (ATR, cm^{-1}): ν 3328s (imidazole proton), 3080w (phenyl proton), 2925w, 1611s (C=C, C=N). 1592vs (C=C, C=N), 1473vs, 1327vs, 827vs. ^{1}H NMR (400 MHz, TMS, DMSO); δ_{ppm} 14.30 (s, 1H, imidazole NH), 9.28 (d, J = 2.7 Hz, 1H), 8.89 (d, J = 8.2 Hz, 2H), 8.54 (d, J = 7.5 Hz, 2H), 8.25 (dd, J = 9.1, 2.7 Hz, 1H), 7.79 (t, J = 7.4 Hz, 2H), 7.71 (t, J = 7.1 Hz, 2H), 7.27 (d, J = 9.1 Hz, 1H). ^{13}C NMR (101 MHz, DMSO) δ 163.32, 128.62, 128.62, 127.98, 127.98, 126.63, 126.63, 124.56, 124.56, 122.49, 122.49, 104.30. MS (EI) m/z 355 (M^+, 100%): 355, 325, 309, 279. Anal. Calc. for $C_{21}H_{13}N_3O_3$: C, 70.98; H, 3.69; N, 11.83%. Found: C, 71.09; H, 3.84; N, 11.14%.

2.3. Preparation of two palladium complexes

2.3.1. Bis-[2-(4,5-diethyl-1H-imidazol-2-yl)phenolato]palladium(II) (***Pd.de*$_2$**)

$Pd(AcO)_2$ (100 mg, 0.45 mmol) and **de** (190 mg, 0.89 mmol) were stirred in EtOH (≈2 mL) at room temperature for 12 h. The precipitate resulting from the reaction was filtered, washed with EtOH (≈2 mL) and dried to afford **Pd.de$_2$** as light green powder. Suitable single crystals for **Pd.de$_2$** were grown by slow evaporation of solvent from its DMF solution (260 mg, 55%). Mp./Dec. > 300 °C. Selected IR peaks (KBr, cm^{-1}): ν 3164 m, 3030 m, 2965s, 1620s, 1595s, 752s. ^{1}H NMR (400 MHz, d6-DMSO): δ 11.16 (s, 1H), 7.25 (d, J = 7.6 Hz, 1H), 6.85 (t, J = 7.8 Hz, 1H), 6.67 (d, J = 8.3 Hz, 1H), 6.39 (t, J = 7.4 Hz, 1H), 3.02 (q, J = 7.4 Hz, 2H), 2.63 (q, J = 7.5 Hz, 2H), 1.23 (t, J = 7.5 Hz, 3H), 1.10 (t, J = 7.0 Hz, 3H) (see supplementary information S2). Anal. Calc. for $C_{26}H_{30}N_4O_2Pd\cdot THF\cdot 2H_2O$: C, 55.86; H, 6.56; N, 8.69%. Found: C, 55.88; H, 6.39; N, 8.95%. TG analysis: 125–145 °C, −14.02% (tightly held solvent or water); 292–307 °C, −78% (ligands).

2.3.2. Bis-[2-(4,5-dimethyl-1H-imidazol-2-yl)-4-nitrophenolato]palladium(II) (***Pd.p-N*∼*dm*$_2$**)

$Pd(AcO)_2$ (53 mg, 0.24 mmol) and ***p*-N∼dm** (111 mg, 0.48 mmol) were reacted under similar manner as for **Pd.de$_2$** to obtain **Pd.*p*-N∼dm$_2$** as orange powder (70 mg, 51%). Mp./Dec. > 300 °C. Selected IR peaks (KBr, cm^{-1}): ν 3271s, 3234s, 3075 m 2929 m, 1627s, 1599s, 1487vs, 1275vs, 753s. Anal. Calc. for $C_{22}H_{20}N_6O_6Pd\cdot HAcO\cdot(1/2)H_2O$: C, 45.05; H, 3.94; N, 13.13%. Found: C, 44.71; H, 3.55; N, 12.84%.

2.4. Suzuki–Myaura coupling catalysis experiments

In typical reactions, (4-bromophenyl)methanol (187 mg, 1.0 mmol) was reacted with 4-acetylphenylboronic acid (197 mg, 1.2 mmol) in DMF/H_2O mixture (3 mL DMF + 1 mL H_2O) as solvent and in the presence of a ligand (0.4% equivalent with respect to arylbromide), palladium(II) acetate (0.2% equivalent with respect to arylbromide) and K_2CO_3 (207 mg, 1.5 mmol). Yields were

obtained by ^{1}H NMR experiments carried out on aliquots drawn from the reaction solution and slowly washed by deuterated chloroform into the NMR tube over a short bed of anhydrous sodium sulphate after 1 h reflux duration. Amount of product resulting from reactions were calculated by comparison of NMR peak integration values for the methanolyl –CH_2– signal on (4-bromophenyl)methanol (the aryl-bromide substrate, $\delta \approx 4.4$ ppm) with that of the biphenyl products ($\delta \approx 4.7$ ppm). The pure catalysis reaction product 1-(4′-(hydroxymethyl)biphenyl-4-yl)ethanone (**1**) was isolated by column chromatography purification on silica gel and characterized by ^{1}H NMR, ^{13}C NMR, elemental analyses and mass spectrometry. Analytical data of aryl-aryl coupled product is as follows: ^{1}H NMR (400 MHz, TMS, $CDCl_3$); δ_{ppm} 8.01 (d, J = 8.0 Hz, 2H); 7.66 (d, J = 8.4 Hz, 2H); 7.61 (d, J = 8.4 Hz, 2H); 7.45 (d, J = 8.0 Hz, 2H); 4.75 (s, 2H, –CH_2–); 2.62 (s, 3H, acetyl). ^{13}C NMR (101 MHz, $CDCl_3$): 197.71 (carbonyl), 141.00, 139.23, 135.92, 128.93, 127.53, 127.45, 127.15, 64.96 (methanolyl), 26.63 (methyl). MS (EI) m/z 226 (M^+, 98%): 226, 211, 165, 152. Anal. Calc. for $C_{15}H_{14}O_2$: C, 79.62; H, 6.24%. Found: C, 79.52; H, 6.31%.

2.5. Experimental probe of donor strengths of imidazole N-base and phenol oxo-atoms

Electronic donor strengths of the ligand donor atoms were accessed *via* their protonation–deprotonation equilibrium constants and the determinations were accomplished spectroscopically by UV–vis measurements done on Shimadzu-1600 Spectrophotometer using $\sim 10^{-5}$ M solutions of the ligands in ethanol–water mixture made up of 70 mL EtOH in 100 mL standard flasks made up to mark with 30 mL H_2O. 0.74 g of KCl was added to each 100 mL standard solution for each compound in order to achieve a KCl concentration of 0.1 M, which is aimed at maintaining a fairly constant ionic strength in the solutions. Adjusting pH of the solutions was achieved by using KOH or HCl solutions under constant stirring by a magnetic stirrer bar. UV measurements were obtained for the ligand solutions under varying pH conditions ranging from ~ pH 0.5 to ~ pH 13.5 and plots of absorbance *vs* pH were made at wavelengths where pH dependent absorbance changes were most significant. The pH of the solution was monitored using a Crison basic 20 pH metre calibrated by buffers of pH 4.0 and 9.2. The pK_a values were extracted from inflection points of the sigmoid fitting done to the absorption *vs* pH scatter with the aid of origin software.

3. Results and discussion

3.1. Syntheses and characterization of the 2-(1H-imidazol-2-yl)phenol compounds

Several bidentate chelators were employed in this investigation because it might aid the understanding the effect of ligand presence and the trends in desirable ligand properties towards providing efficient palladium active sites. As presented in Scheme 1(a)–(c), ligands under investigation can be conveniently grouped into three series on the basis of bulky nature; the least sterically demanding being the 4,5-dimethyl (~**dm**) and the 4,5-diethyl (~**de**) members (Scheme 1(a)) while the bis-imidazole (**Bis-im**) and phenanthreneyl (~**pt**) analogues (***o,p-t*Bu~pt**, **m-M~pt** and ***p*-N~pt**) represent the bulky/rigid ligand frameworks (Scheme 1(c)). Ligands of the 2-(4,5-diphenyl-1H-imidazol-2-yl)phenol (**dp**) series (Scheme 1(b)) are considered to be between these two extremes of bulkiness/flexibility. Within each of the three groups, diversity of electronic character was the basis for the choice of substituents. Therefore, substituents were systematically positioned *para* to the phenol hydroxyl group in order to produce electron push or withdrawing effects towards the oxo-donor atom or positioned *ortho* to the hydroxyl group in order to probe steric effects as well as electronic influences. Synthetic data for these compounds are consistent with the identity of the intended molecules [53–55]. It is noteworthy that the 4,5-dialkyl-substituted imidazole ligands (Scheme 1(a)) prepared from 2,3-butadione or 3,4-hexandion give lesser yields compared to those prepared from benzil. As a result, obtaining pure ligands for the 4,5-dialkyl-substituted imidazole ligands attracts purification by chromatography on silica gel while some of the 4,5-dipheny-substituted imidazole compounds give yields that are high enough to permit only recrystallization from suitable solvents. This observation is attributed to undesirable reaction paths suffered by the 2,3-butadione or 3,4-hexandion reagent.

Occurrence of adduct solvent molecules as indicated by the NMR, FTIR, elemental analyses and even X-ray characterization data is a phenomenon usually observed for azole compounds and they are often present in non-stoichiometric amounts in air- or oven-dried samples [50–56]. In fact, it is rare to find single crystal structures of azole-based ligands or complexes without hydrogen-bonded solvent adducts or intermolecular networks. This is especially so if the imidazole proton is unsubstituted. As reported for the synthesis of ligand **de**, the acetic acid adduct molecule bonded to **de** is so tightly held that it remains intact after passage on silica gel during purification [53]. ^{1}H NMR spectra of the ligands show varying amounts of ethyl acetate, water, acetic acid, *etc.*, relative to ligand signals (see supplementary information S1). Even the three crystal structures herein reported show diverse behaviours of solvent adduct inclusion.

The ability of the explored ligands to form bis-ligated complexes with palladium(II) ion in high yield has been established through the preparation of the complex of **de** as representative for comparison of catalytic outcome for active species generated from the 'ligand + palladium(II) salt' approach with the catalyst obtained from the corresponding preformed palladium complex. $Pd(N\hat{O})_2$ complexes possess saturated coordination environment with coordination number four. Therefore, prior dissociation of ligand donors from some of the metal coordination sites under high temperature Suzuki–Miyaura catalytic condition is necessary to generate active species. Thus, it is anticipated that active species obtained during breakdown may also be built up *in situ* from reaction of palladium(II) salt with ligands at the catalysis temperature (Scheme 2(a)).

3.2. X-ray analyses for p-N~de, p-tBu~dp and ***Pd.de*$_2$**

Single crystal samples of ***p*-N~de**, ***p-t*Bu~dp** and **Pd.de$_2$** suitable for X-ray analysis were respectively grown from their ethyl acetate, ethanol and dimethylformamide solutions by slow evaporation. Data for their structural refinement processing parameters are presented in supplementary information Table S1. While ***p*-N~de** crystallizes in monoclinic Cc space group, both ***p-t*Bu~dp** and **Pd.de$_2$** crystallize in the triclinic P-1 space group. The observed occurrence of hydrogen-bonded solute-solvent/solute-solute interactions in all the structures gives support to the conclusion on presence of adduct molecules as reflected in the analytical characterization data of the synthesized compounds (Figs. 1–3).

A very key observation in the structural data for ***p*-N~de** is the substituent-induced intramolecular proton-electron rearrangement. The withdrawal of O—H bonding electrons towards the nitro-substituted aryl ring leads to carbonyl double bond character of the C—O bond (1.300(4) Å), perturbation of the aromaticity of the supposed phenol ring and a compensatory transfer of the phenolic proton to the imidazole ring (Scheme 2(b)). This observation is a direct consequence of the presence of electron withdrawing nitro-substituent on the phenol ring of ***p*-N~de**. Therefore, the structural

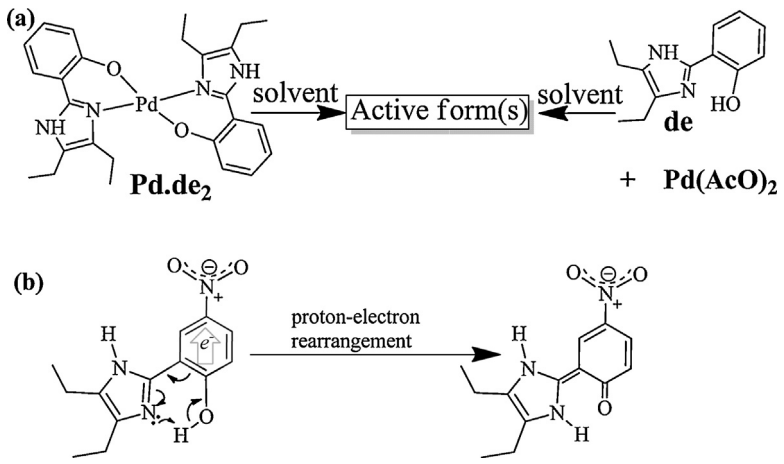

Scheme 2. (a) Hypothetical routs to palladium active forms *via* high temperature disassembly of the Pd(NÔ)$_2$ complex or by assembly from 'ligand + palladium salt'. (b) Observed structural character induced by nitro substituent.

result for ligand ***p*-N∼de** suggests that the strength of interaction of the ligand as anion with Pd^{2+} would be largely dependent on heterocyclic imidazolate nitrogen donor and a weak or no interaction from the oxo-atom; *i.e.* this is a display of significant tendency for monodentate coordination based on an anionic imidazole. An evidence for this conclusion has been seen with a *para*-bromo-substituted imidazole-phenol complex in which the only remaining coordination site on the palladium ion bonds to the imidazole nitrogen base while the phenol oxo donor abstains from coordination.

It is expected that the absence of strong electron-withdrawing influence at the *para*-position would cause a phenolate oxygen atom to be the anionic arm of the bidentate ligand framework while the imidazole nitrogen base would play a complimentary neutral donor role which could be fairly strong too. The transfer of acetic acid proton to the imidazole nitrogen base of ***p*-*t*Bu∼dp** (Fig. 2) and the stability of the acetate-imidazolium product formed even after passage over silica gel during column chromatography indicated a fairly reliable donor strength of the imidazole nitrogen base of ***p*-*t*Bu∼dp**. Thus, a bidentate chelate coordination character would be anticipated for such ligand frameworks. Furthermore, this bidentate character is expected to be enhanced in the presence of electron inducing group like *tert*-butyl at the *para*-position. While the structure of ***p*-N∼de** revealed the proton-electron rearrangement as a consequence of the presence of nitro group, structural data for the ligand ***p*-*t*Bu∼dp** is in accordance with a stable phenol-aromatic electronic situation. Supplementary information Table S2 presents summary of selected corresponding bond lengths for comparison from ***p*-N∼de** and ***p*-*t*Bu∼dp**. The active protons for the two ligands were picked on the difference map during refinement and not fixed. Comparing the bond lengths for the phenolic moieties of the two ligand structures indicates that aromaticity is intact for ***p*-*t*Bu∼dp** while ***p*-N∼de** showed bond lengths for C(1)–C(6) (1.446(4) Å) tending towards single bond character. The imidazole bond lengths C(7)–N(1) and C(7)–N(2) are more or less equal for ***p*-*t*Bu∼dp** as should be expected for an imidazolium ring after

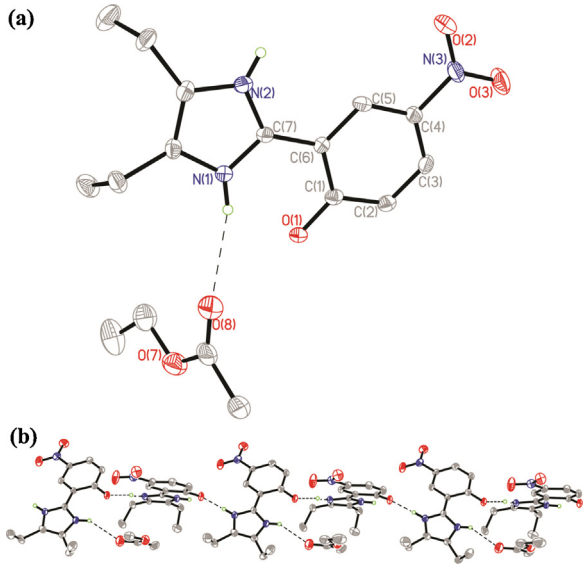

Fig. 1. Ortep plot of (a) ***p*-N∼de.EtAcO** and (b) its 1-dimensional network; thermal ellipsoids drawn at the 50% probability level. Some atomic labels and protons have been omitted for clarity.

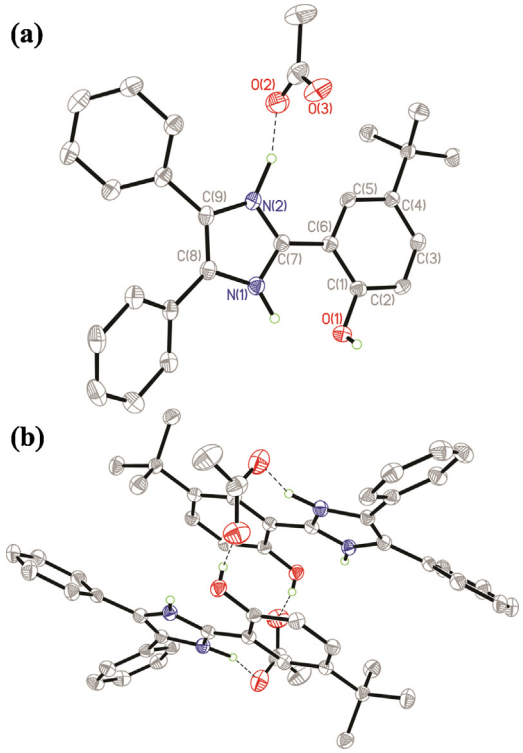

Fig. 2. Ortep plot of (a) ligand ***p*-tBu∼dp.HAcO** and (b) its dimer stack enhanced by acetic acid. Thermal ellipsoids are drawn at the 50% probability level. Some atomic labels and protons have been omitted for clarity.

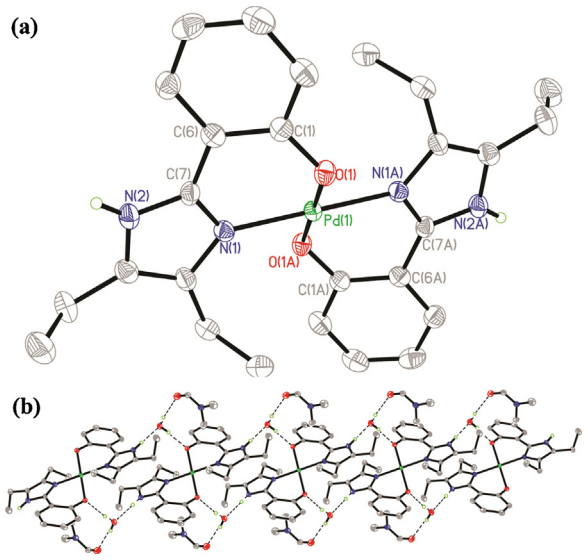

Fig. 3. Ortep plot of (a) **Pd.de$_2$** and (b) its 1D-network mediated by hydrogen-bonded water and dmf. Thermal ellipsoids are drawn at the 50% probability level. Some atomic labels, protons and solvent molecule have been omitted for clarity.

transfer of the acetic acid proton, but the difference in the bond lengths C(7)–N(1) and C(7)–N(2) for ***p*-N∼de** is in agreement with the suggested electron-proton rearrangement.

It is noteworthy that the acetate-imidazolium association as presented in the structure of ***p*-*t*Bu∼dp** survived neutralization of the acetic acid preparation medium by concentrated ammonium hydroxide solution, recrystallization of its crude synthetic product from hot ethyl acetate and growing of its single crystals from ethanol. This indicates fairly strong donor strength of its imidazole N-base. Furthermore, the observed dimerization of the imidazolium-acetate units is aided by face-to-face π-stacking interactions between the aromatic rings on the ligands (∼ 3.340 Å). The R-factor of 10% for the crystal data of ***p*-*t*Bu∼dp** came about as a result of disordered free solvent molecules.

In the case of **Pd.de$_2$**, the green crystalline needles grown from DMF were found to contain a 1-dimentional network made possible by solvent-mediated hydrogen-bonding interactions between bis-ligated palladium complex units. Each complex unit is held to the next at two points *via* bridging water molecules, which were observed to be bridging between the imidazole proton on one complex and the phenolate oxygen on the next complex. DMF molecules were also found to be hydrogen-bonded to each of these water molecules (Fig. 3).

3.3. Investigation of influence of ligand presence in palladium catalyzed Suzuki–Miyaura cross-coupling

The series of ligands were subjected to the catalytic experiments under the same reaction conditions involving (4-bromophenyl)methanol (1.0 mmol), 4-acetylphenylboronic acid (1.2 mmol), K_2CO_3 (1.5 mmol), DMF/H_2O solvent mixture (3 mL DMF, 1 mL H_2O), palladium(II) acetate (0.2 mol%), ligand (0.4 mol%) and under 1 h reflux (Scheme 3). The suitability of catalytic substrates and reaction conditions were decided based on optimum

Table 1
Estimation of catalytic turnover frequencies.

Entry	Catalyst system	Yield[a] (%)	TON
1	**Pd(AcO)$_2$**	29	145
2	**Pd(AcO)$_2$ + *p*-*t*Bu∼dm**	17	85
3	**Pd(AcO)$_2$ + de**	16	80
4	**Pdde$_2$**	35	175
5	**Pd(AcO)$_2$ + *p*-M∼dm**	06	30
6	**Pd(AcO)$_2$ + *p*-N∼dm**	52	260
7	**Pd.*p*-N∼dm$_2$**	69	345
8	**Pd(AcO)$_2$ + *p*-N∼de**	90	450
9	**Pd(AcO)$_2$ + *o*-*t*Bu∼dp**	13	65
10	**Pd(AcO)$_2$ + *o*,*p*-*t*Bu∼dp**	06	30
11	**Pd(AcO)$_2$ + *o*,*p*-Dm∼dp**	06	30
12	**Pd(AcO)$_2$ + dp**	33	166
13	**Pd(AcO)$_2$ + *o*-H∼dp**	20	100
14	**Pd(AcO)$_2$ + *o*-M∼dp**	22	110
15	**Pd(AcO)$_2$ + *p*-Br∼dp**	56	280
16	**Pd(AcO)$_2$ + *p*-N∼dp**	46	230
17	**Pd(AcO)$_2$ + *o*,*p*-N∼dp**	74	370
18	**Pd(AcO)$_2$ + *o*,*p*-*t*Bu∼pt**	32	160
19	**Pd(AcO)$_2$ + *m*-M∼pt**	06	30
20	**Pd(AcO)$_2$ + *p*-N∼pt**	74	370
21	**Pd(AcO)$_2$ + Bis-Im**	13	65

[a] Reactions conditions: (4-bromophenyl)methanol (1.0 mmol), 4-acetylphenylboronic acid (1.2 mmol), K_2CO_3 (1.5 mmol), DMF/H_2O solvent mixture (3 mL DMF, 1 mL H_2O), palladium(II) acetate (0.2% of arylbromide) and ligand (0.4% of arylbromide), 1 h reflux. Yields were obtained by ^{1}H NMR peak integration comparison of aryl-bromide substrate ($\delta \approx 4.5$ ppm) and biphenyl products ($\delta \approx 4.7$ ppm).

conditions observed in recently documented study, which involved a series of dichloropalladium(II) complexes of neutral 2-(1H-imidazol-2-yl)pyridines [59]. In particular, the –CH_2– (methylene) function on the (4-bromophenyl)methanol substrate enables ease of ^{1}H NMR tracking of substrate conversion to coupled product. This functional group was found to be advantageous because there is no interference around the 4.5 ppm ^{1}H NMR region where –CH_2– group of the –CH_2OH substituent gives signal [59]. Furthermore, we have recently investigated dependence of catalytic outcomes on varying amounts of reactants, base additives and solvents as well as dependence on the application of varying types of base additive, arylbromides, arylboronic acids, reaction atmospheres (air and N_2), reflux durations and catalyst loadings [59]. Findings in these recent experiments informed the basis for considering that 1.5 mole equivalent of K_2CO_3, dimethylformamide/water mixture (3:1, 4 mL), arylbromide:arylboronic acid ratio of 1:1.2, catalyst loading of 0.2 mol. % and 1hr reflux would be adequate in this study. Yields were obtained by ^{1}H NMR comparison of integration values for methylene (–CH_2–) signal of the methanolyl group on (4-bromophenyl)methanol ($\delta \approx 4.4$ ppm) with that of the cross-coupling product ($\delta \approx 4.7$ ppm). Results obtained are presented in Table 1. The choice of the applied reaction conditions is aimed to enable discrimination in the catalytic outcomes on the bases of the presence of different chelate frameworks.

Comparing catalytic results for the reactions in which there is presence of one of the ligands with the reaction carried out with only palladium acetate (Table 1, Entry 1), the turnover number values (TON) indicate that ligands play some role in influencing activity of the metal active centre. A key feature of the ligand effect in the catalytic results summarized in Table 1 is that ligands bearing electron withdrawing substituent at the *para*-position to

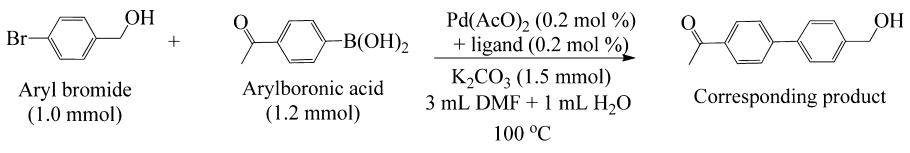

Scheme 3. The cross-coupling reaction carried out.

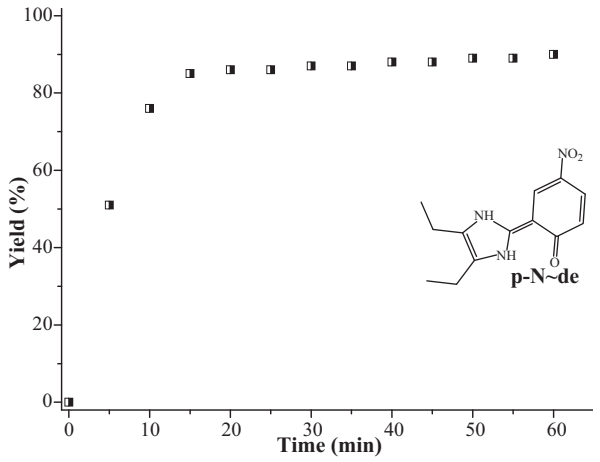

Fig. 4. Plot of yield against time for catalysis in the presence of ***p***-N~de.

the phenolic hydroxyl oxo-atom yielded more positive influence to the cross-coupling reaction. In particular, higher TON values were achieved after 1 h reflux in the presence of ***p*-N~de** (TON = 450, yield = 90%, Entry 7), ***o,p*-N~dp** (TON = 370, yield = 74%, Entry 14) and ***p*-N~pt** (TON = 370, yield = 74%, Entry 19) compared with result for the same catalysis reaction in the presence of only palladium acetate as catalyst (TON = 145, yield = 29%, Entry 1). Furthermore, only ligands possessing electron withdrawing functions on the phenol ring produced yields higher than 45% within the 1 h reflux time; *i.e.* ***p*-N~dm** (TON = 260, yield = 52%, Entry 6), ***p*-Br~dp** (TON = 280, yield = 52%, Entry 15) and ***p*-N~dp** (TON = 230, yield = 46%, Entry 16). Since apparent deactivation of the phenol –OH group towards coordination appears to be favourable for the catalysis, it may be reasonable to infer that the palladium species possessing superior catalyst efficiencies in the investigated series bear the ligands in a monodentate fashion involving an anionic imidazolate donor. This view is strengthened by the fact that electron-inducing substitution in place of the nitro- or bromo-substituents does not only result in low yields, but also appear to poison the palladium catalyst (Entry 1 *vs* Entries 2, 5, 10, 11, 18 and 19), which may be attributed to the higher bidentate chelate character due to stronger availability of both phenolate oxo-atom and imidazole nitrogen donors for coordination. It is worthy of note that methoxy groups also display electron richness. In order to examine catalytic efficiencies of active species generated by *in situ* reaction of Pd(II) with representative members of the different electronic classes of the ligands against catalytic efficiencies obtainable from their corresponding preformed Pd complexes, **Pd.de$_2$** and **Pd.*p*-N~dm$_2$** were employed as catalyst under similar reaction conditions. It was observed that the preformed complex **Pd.de$_2$** yielded higher catalytic efficiency compared to the *in situ* approach, but with efficiency comparable to catalysis in the presence of only palladium acetate (Entry 3 *vs* Entry 4). **Pd.*p*-N~dm$_2$** (TON = 345, yield = 69, Entry 7) also gave a slightly improved performance relative to data obtained from '**Pd(AcO)$_2$ + *p*-N~dp**' catalyst system (TON = 260, yield = 52%, Entry 6), but the difference may not justify a necessity for prior synthetic procedures for the complex.

In order to make a kinetic assessment of the highest performing ligand, aliquots of reaction mixture were taken at 5 min intervals up to 60 min for estimation of amount of product formed in the presence of palladium acetate and ***p*-N~de**. The plot of yield against time is presented in Fig. 4 and it shows that initial rate within the first 10 min of the catalysis is high until about 80% yield. Afterwards, the rate reduces significantly, which may be attributed to the large extent to which reactants have disappeared. Comparing catalytic results on the basis of ligand steric/rigid factors especially with the ligands that contribute positive catalytic influence, it could be concluded that the electronic character of the ligands hold a higher importance above their directional properties. Relative to catalysis results in the presence of ***p*-N~de**, lower yields obtained for ***p*-N~dm** (*i.e.* with smaller 4,5-methyl imidazole-substituent fragments) or ***p*-N~dp**, ***o,p*-N~dp** and ***p*-N~pt** (*i.e.* with larger 4,5-phenyl/phenanthrenelyl imidazole-substituent fragments) suggest the existence of a safe magnitude of steric environments that should be provided by the ligands around the palladium site for increased efficiency (Table 1: Entry 8 *vs* Entry 6 on the one hand and *vs* Entries 15, 16, 17 and 18 on the other hand). It is important to realize that if the proposed coordination of only the imidazole part of the favourable ligands is in effect, the phenoxo moiety will also constitute a steric bulk around the palladium centre. Thus, further increasing steric bulk in the 4,5-imidazole direction has produced undesirable effects. Furthermore, the view that electronic character is more relevant relative to steric character is supported by the fact that the presence of the dinitro-substituted ***o,p*-N~dp** in the catalysis mixture yielded better result than for the mononitro-substituted counterpart ***p*-N~dp** despite that the former would suffer a more steric effect contribution from the additional *ortho*-nitro- group (Table 1: Entry 17 *vs* Entry 16). The planar phenanthreneyl attachment to the 4,5-imidazole carbons of ***p*-N~pt**, though more rigid, happens to display lesser steric demands compared to its 4,5-diphenyl analogue ***p*-N~dp** (Table 1: Entry 20 *vs* Entry 16).

3.4. Experimental and theoretical probe of ligands' electronic/donor characters

Use of UV spectroscopic method in quantifying changing concentrations of equilibrium species in a solution is known to render reliable results and the ionization constants can be obtained as pK_a on the basis of Henderson–Hasselbalch equation [58]:

$$\mathrm{pH} = \mathrm{p}K_a - \log \frac{A - A_0}{A_f - A}$$

A_0 and A_f represent the absorbance values at a given wavelength when the solute molecules are totally on one side of a particular pair of protonated–deprotonated forms for a given equilibrium. A represents absorbance value of the protonation-deprotonation equilibrium mixtures at the same wavelength, but under varying pH. The pK_a values were obtained from non-linear least square sigmoid fittings on plots of pH against absorbance values at a selected wavelength (inset of Figs. 5 and 6). R^2 values are all around 99%.

Considering the protonation-deprotonation events illustrated in Scheme 4, spectroscopic experiments were carried out to calculate equilibrium constants derived as pK_as in order to determine protonation ease or otherwise for the ligands prepared during this work. The pK_as for our previously prepared ligands have been documented [51,54] while Table 2 contains a summary of the presently and previously estimated pK_as. Examples of the spectral stack diagrams for the investigated compounds are presented in Figs. 4 and 5 with inset of sigmoid fittings on plots of absorbance against pH. The pH value at the point of inflection is equal to the pK_a for a given protonation-deprotonation equilibrium. The UV spectral stacks displayed clear isosbetic points, which shows that spectral absorbance heights were changing only due to changes in electronic state of solute species rather than due to overall change in concentration of the solute ligands. Due to complicated spectral traces, it was not possible to obtain useful pH dependent spectral profiles for the nitro-substituted ligands ***p*-N~dm**, ***p*-N~de**, ***p*-N~dp** and ***o,p*-N~dp**. This observation is attributed to occurrence of more than one protonation-deprotonation equilibrium set up at the nitro-function, which simultaneously responding to pH change during addition of acid or base. Protonation of the imidazole N-base

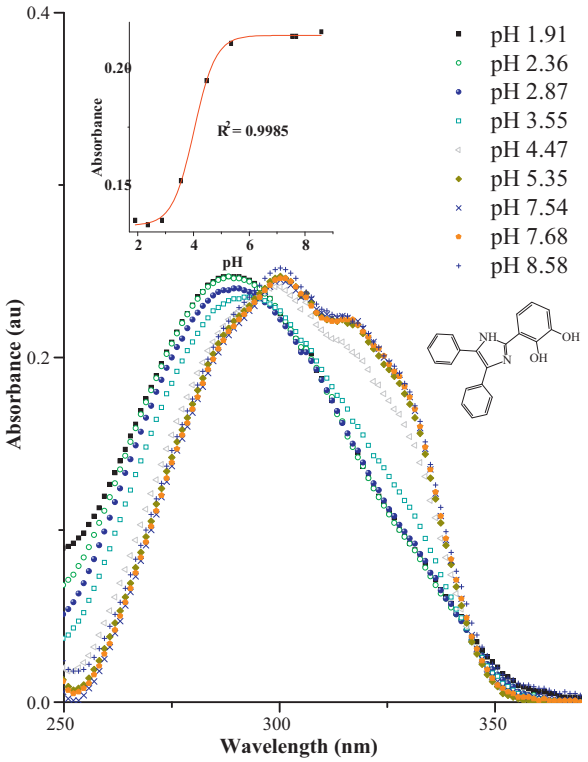

Fig. 5. Spectral overlays for ***o***–H~dp in the acidic pH range showing isosbetic points; inset is sigmoid plot of absorbance *vs* pH.

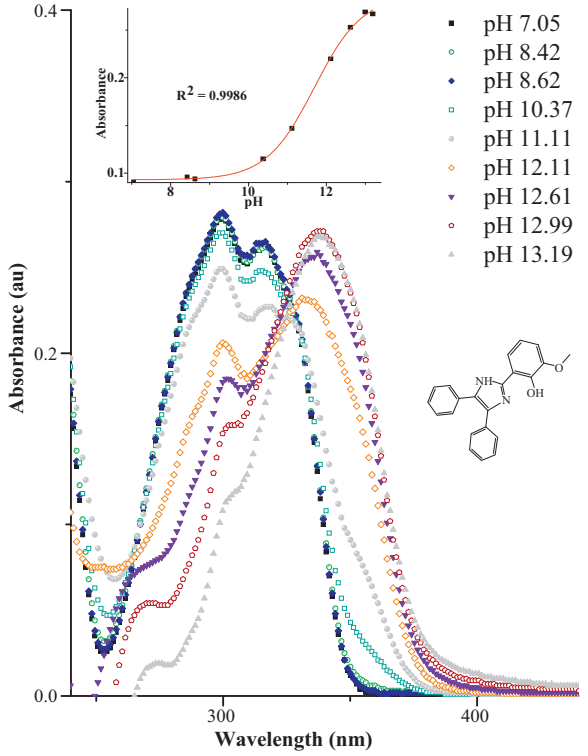

Fig. 6. Spectral overlays for ***o***–M~dp under alkaline pH showing isosbetic points; inset are sigmoid plot of absorbance *vs* pH.

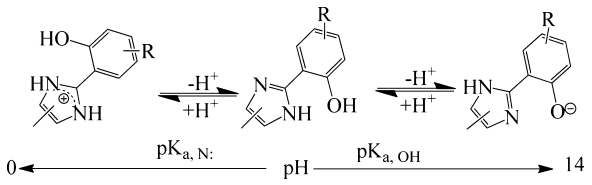

Scheme 4. Protonation–deprotonation equilibria for the NÔ ligands.

was achieved by addition of acid while deprotonation of the active protons require addition of base. Based on previous experiments involving 2-(1H-imidazol-2-yl)pyridines [50], deprotonation of the imidazole proton under the alkaline pH range can be ruled out and the observed pK_as in the alkaline pH experiments are attributed to deprotonation of the phenolic –OH active proton.

The higher the pK_a value for the imidazole N-base protonation ($pK_a^{N:}$) or phenolic OH (pK_a^{OH}), the higher the donor capacity of the N-base or phenolate lone pairs and *vice versa.* Literarily, higher $pK_a^{N:}$ for imidazole protonation implies that it is easier to saturate the imidazole N-base with protons at higher pH rather than requiring much addition of H^+ concentrations for lower pH. On the other hand, higher pK_a^{OH} values would imply that higher alkalinity concentration (*i.e.* higher pH) would be required for detachment of corresponding hydroxyl active proton. From the results summarized in Table 2, higher pK_a^{OH} values (hydroxyl deprotonation) observed with the *t*-Bu-substituted ligand frameworks relative to others is consistent with the conclusion of stronger donor character of their oxo-atoms (See pK_a^{OH} for Entries 1, 6, 7 and 15 *vs* other entries). Furthermore, within the 4,5-diphenyl-imidazole series, their pK_a^{OH} values reduced as electron inducing strength of the phenol ring substituents reduced; ***o,p-t*Bu~dp** [13.47 (±0.02)] ≈ ***p-t*Bu~dp** [≥13.32 (±0.14)] > ***o,p*-Dm~dp** [≥11.64 (±0.09)] > **dp** [≥10.05 (±0.08)]. Therefore, the agreement between higher pK_a^{OH} values (*i.e.* strong oxo-donor strengths) and the corresponding low yields or catalyst poisoning behaviours support the thinking that strong bidentate chelation

Table 2
Experimentally estimated acid/base strengths of the imidazole ligand derivatives (obtained as pK_as).[a]

Entry	Ligands	Free ligand deprotonation constants[g]	
		$pK_a^{N:}$ (±S)[b]	pK_a^{OH} (±S)
1	***p-t*Bu~dm**	–[f]	>14.00[c]
2	**de**	6.64 (±0.07)[d]	11.91 (±0.10)[d]
3	***p*-M~dm**	6.62 (±0.15)	12.26 (±0.07)
4	***p*-N~dm**	–[f]	–[f]
5	***p*-N~de**	–[f]	–[f]
6	***o-t*Bu~dp**	≤2.01 (±0.05)[c]	≥13.32 (±0.14)[c]
7	***o,p-t*Bu~dp**	2.28 (±0.04)[d]	13.47 (±0.02)[d]
8	***o,p*-Dm~dp**	3.38 (±0.07)[d]	11.64 (±0.09)[d]
9	**dp**	4.22 (±0.10)[d]	10.05 (±0.08)[d]
10	***o*-H~dp**	4.02 (±0.03)	10.18 (±0.02)
11	***o*-M~dp**	3.54 (±0.05)	11.69 (±0.06)
12	***p*-Br~dp**	3.27 (±0.11)	10.36 (±0.05)
13	***p*-N~dp**	–[f]	–[f]
14	***o,p*-N~dp**	–[f]	–[f]
15	***o,p-t*Bu~pt**	1.11 (±0.02)[d]	13.04 (±0.08)[d]
16	***m*-M~pt**[e]	3.37 (±0.03)[e]	11.33 (±0.11)[e]
17	***p*-N~pt**	–[f]	–[f]
18	**Bis-Im**	Not done	Not done

[a] Obtained spectroscopically.
[b] ±S represents standards errors.
[c] These are approximate pK_as since their sigmoid fittings are non-symmetrical for extreme of pH data.
[d] Data according to Ref. [42].
[e] Data according to Ref. [45].
[f] Complicated spectral profile at various pH prevented calculation of pK_as.
[g] The pK_a data were determined in an independent experiment and not in the presence of palladium acetate.

adversely affected the palladium efficiency and that monodentate imidazolate coordination in the presence of poor donor oxo-atoms is proposed to be beneficial for the cross-coupling event. The pK_a^N: values pertaining to the imidazole base donor strength did not give a clear trend in correlation with catalytic role of the ligands, but the crystal data for the diethyl- and dephenyl-ligands presented above suggests that the imidazole donor strengths are generally fairly strong regardless of 4,5-imidazole substitution.

DFT calculations using B3LPY/6311+G* were carried out to optimize the geometries of all studied ligands under simulated water/ethanol dielectric constant in effort to further pursue understanding of the peculiar characteristics common to the ligands that displayed favourable ligand effects towards *in situ* generation of active species. Unfortunately, there was no clear correlation between experimentally observed trends and the theoretically derived Mullekan charges on the ligand donor atoms. Thus, the data is not presented.

4. Conclusion

Series of 2-(1H-imidazol-2-yl)phenol ligand members synthesized and properly characterized were employed in catalytic studies aimed to improve understanding of favourable ligand characteristics for *in situ* generation of palladium active species towards Suzuki–Miyaura coupling reaction. The potential of the bidentate ligand series to form bis-ligated $Pd(N\hat{O})_2$ complex types was established. Structures of ligands 2-(4,5-diethyl-1H-imidazol-2-yl)-4-nitrophenol (***p*-N∼de**) and 4-(tert-butyl)-2-(4,5-diphenyl-1H-imidazol-2-yl)phenol (***p*-*t*Bu∼dp**) as well as the bis-ligand palladium complex (**Pd.de$_2$**) of 2-(4,5-diethyl-1H-imidazol-2-yl)phenol (**de**) were confirmed by single crystal X-ray crystallography. Crystal data information revealed that nitro-substituted phenol moieties bear poor donor oxo-atoms while the reverse was observed for *tert*-butyl substituted phenol. Donor strengths of the phenolic oxo-atoms and the imidazole N base were also experimentally determined as pK_as by protonation-deprotonation equilibrium studies using UV spectroscopy.

Under the same reaction conditions for palladium catalyzed Suzuki–Miyaura coupling of (4-bromophenyl)methanol and 4-acetylphenylboronic acid, all the ligands were tested for ligand-presence effects towards *in situ* generation of palladium active sites (*i.e.* from 'ligand + palladium(II) acetate' catalyst approach). The same catalysis experiment was also conducted in the presence of only palladium acetate and the results compared. The results show that electronic properties of the ligands are more important deciding factors than the variation in steric properties in this ligand series. In particular, ligands with strong bidentate chelate coordination potentials (*e.g. tert*-butyl-substituted phenol analogues) acted as poisons while those with monodentate coordination potential (*i.e.* the nitro-substituted phenol ligands) proved to be very beneficial towards *in situ* generation of superior active species. Furthermore, the agreement between higher pK_a^{OH} values (*i.e.* strong oxo-donor strengths) and the corresponding low yields or catalyst poisoning behaviours from ligands with *tert*-butyl-substituted phenol rings support the conclusion that ligands with strong chelation tendencies adversely impacted the efficiency of *in situ* palladium catalyst generation and that monodentate imidazolate coordination in the presence of poor donor phenolic oxo-atoms is likely to be the configuration of the superior active species in the studied series.

Supplementary information

CCDC 882515, 886818 and 960988 contains the supplementary crystallographic data for *p*-*t*Bu∼dp and **Pd.de$_2$**. These data can be obtained free of charge *via* www.ccdc.cam.ac.uk/data_request/cif from the Cambridge Crystallographic Data Centre.

Acknowledgements

A.O.E is grateful to the Redeemer's University Research Grants Committee for supports towards purchase of some laboratory facilities. The authors are also thankful for generous grants from the Deutsche Forschungsgemeinschaft (DFG: PL 155/9, PL 155/11, and PL 155/12).

Appendix A. Supplementary data

Supplementary data associated with this article can be found, in the online version, at http://dx.doi.org/10.1016/j.molcata.2014.02.032.

References

[1] H. Jacobsen, A. Correa, A. Poater, C. Costabile, L. Cavallo, Coord. Chem. Rev. 253 (2009) 687–703.
[2] K.A. Netland, A. Krivokapic, M. Schröder, K. Boldt, F. Lundvall, M. Tilset, J. Organomet. Chem. 693 (2008) 3703–3710.
[3] E. Ullah, J. McNulty, A. Robertson, Tetrahedron Lett. 50 (2009) 5599–5601.
[4] H. Doucet, J.-C. Hierso, Angew. Chem. Int. Ed. 46 (2007) 834–871.
[5] T.E. Barder, S.L. Buchwald, Org. Lett. 6 (2004) 2649–2652.
[6] S.T. Marshall, M. O'Brien, B. Oetter, A. Corpuz, R.M. Richards, D.K. Schwartz, J.W. Medlin, Nat. Mater. 9 (2010) 853–858.
[7] T. Thaler, B. Haag, A. Gavryushin, K. Schober, E. Hartmann, R.M. Gschwind, H. Zipse, P. Mayer, P. Knochel, Nature Chem. 15 (2010) 125–130.
[8] M. Lamblin, L. Nassar-Hardy, J.-C. Hierso, E. Fouquet, F.-X. Felpin, Adv. Synth. Catal. 352 (2010) 33–79.
[9] J.G. de Vries, Dalton Trans. 2006 (2006) 421–429.
[10] A.S. Guram, X. Wang, E.E. Bunel, M.M. Faul, R.D. Larsen, M.J. Martinelli, J. Org. Chem. 72 (2007) 5104–5112.
[11] A. Suzuki, Tetrahedron Lett. 22 (1981) 127–130.
[12] N. Miyaura, K. Yamada, A. Suzuki, Tetrahedron Lett. 20 (1979) 3437–3440.
[13] E. Negishi, H. Matsushita, N. Okukado, Tetrahedron Lett. 22 (1981) 2713–2715.
[14] E. Negishi, H.-J. Matsushita, M. Kobayashl, C.L. Rand, Tetrahedron Lett. 24 (1983) 3823–3824.
[15] E. Negishi, T. Takahashi, K. Akiyoshi, J. Organomet. Chem. 334 (1987) 181–194.
[16] H.A. Dieck, F.R. Heck, J. Organomet. Chem. 93 (1975) 259–263.
[17] M. Qian, E. Negishi, Tetrahedron Lett. 46 (2005) 2927–2930.
[18] M. Miura, Angew. Chem. Int. Ed. 43 (2004) 2201–2203.
[19] R. Chinchilla, C. Najera, Chem. Rev. 107 (2007) 874–922.
[20] N. Miyaura, A. Suzuki, Chem. Rev. 95 (1995) 2457–2483.
[21] E.A.B. Kantchev, C.J. O'Brien, M.G. Organ, Angew. Chem. Int. Ed. 46 (2007) 2768–2813.
[22] E. Peris, R.H. Crabtree, Coord. Chem. Rev. 248 (2004) 2239–2246.
[23] A.F. Littke, G.C. Fu, Angew. Chem. Int. Ed. 41 (2002) 4176–4211.
[24] Z. Weng, S. Teo, T.S.A. Hor, Acc. Chem. Res. 40 (2007) 676–684.
[25] G. Shore, S. Morin, D. Mallik, M.G. Organ, Chem. A: Eur. J. 14 (2008) 1351–1356.
[26] N.T.S. Phan, M. VanDerSluys, C.W. Jones, Adv. Synth. Catal. 348 (2006) 609–679.
[27] T.I. Wallow, B.M. Novak, J. Org. Chem. 59 (1994) 5034–5037.
[28] T. Takemoto, S. Iwasa, H. Hamada, K. Shibatomi, M. Kameyama, Y. Motoyamac, H. Nishiyama, Tetrahedron Lett. 48 (2007) 3397–3401.
[29] F. Amorosoa, S. Colussia, A.D. Zotto, J. Llorca, A. Trovarelli, J. Mol. Cat. A: Chem. 315 (2010) 197–204.
[30] J.A. Widegren, R.G. Finke, J. Mol. Catal. A: Chem. 198 (2003) 317–341.
[31] E.R. Strieter, D.G. Blackmond, S.L. Buchwald, J. Am. Chem. Soc. 125 (2003) 13978–13980.
[32] S.D. Walker, T.E. Barder, J.R. Martinelli, S.L. Buchwald, Angew. Chem. 116 (2004) 1907–1912.
[33] D. Astruc, Inorg. Chem. 46 (2007) 1884–1894.
[34] D.N. Korolev, N.A. Bumagin, Tetrahedron Lett. 47 (2006) 4225–4229.
[35] D. Astruc, Organometallic Chemistry and Catalysis, 1st ed., Springer, Berlin/Heidelberg/New York, 2007 (Ch. 20).
[36] M. Cai, Q. Xu, Y. Huang, J. Mol. Catal. A 271 (2007) 93–97.
[37] P.D. Stevens, G. Li, J. Fan, M. Yen, Y. Gao, Chem. Commun. 2005 (2005) 4435–4437.
[38] W. Chen, C. Xi, Y. Wu, J. Organomet. Chem. 692 (2007) 4381–4388.
[39] J. Ruiz, C. Vicente, N. Cutillas, J. Pérez, Dalton Trans. 2005 (2005) 1999–2006.
[40] A. Kumar, M. Agarwal, A.K. Singh, J. Organomet. Chem. 693 (2008) 3533–3545.
[41] E. Tas, A. Kilic, M. Durgun, I. Yılmaz, I. Ozdemir, N. Gurbuz, J. Organomet. Chem. 694 (2009) 446–454.
[42] C.-Y. Liao, K.-T. Chan, C.-Y. Tu, Y.-W. Chang, C.-H. Hu, H.M. Lee, Chem. Eur. J. 15 (2009) 405–417.
[43] T.E. Barder, S.D. Walker, J.R. Martinelli, S.L. Buchwald, J. Am. Chem. Soc. 127 (2005) 4685–4696.
[44] D. Bradley, G. Williams, M.L. Shaw, Tetrahedron 63 (2007) 1624–1629.
[45] F. Lepifre, S. Clavier, P. Bouyssou, G. Coudert, Tetrahedron 57 (2001) 6969–6975.
[46] S.A. Patil, C.-M. Weng, P.-C. Huang, F.-E. Hong, Tetrahedron 65 (2009) 2889–2897.
[47] S. Kotha, K. Lahiri, D. Kashinath, Tetrahedron 58 (2002) 9633–9695.

[48] R. Martin, S.L. Buchwald, Acct. Chem. Res. 41 (2008) 1461–1473.
[49] W. Yang, C. Liu, J. Qiu, Chem. Commun. 46 (2010) 2659–2661.
[50] A.O. Eseola, W. Li, O.G. Adeyemi, N.O. Obi-Egbedi, J.A.O. Woods, Polyhedron 29 (2010) 1891–1901.
[51] A.O. Eseola, N.O. Obi-Egbedi, Spectrochim. Acta A: Mol. Biomol. Spec. 75 (2010) 693–701.
[52] A.O. Eseola, W.-H. Sun, W. Li, J.A.O. Woods, J. Mol. Struct. 984 (2010) 117–124.
[53] A.O. Eseola, W. Li, R. Gao, M. Zhang, X. Hao, T. Liang, N.O. Obi-Egbedi, W.-H. Sun, Inorg. Chem. 48 (2009) 9133–9146.
[54] A.O. Eseola, O. Adepitan, H. Görls, W. Plass, New J. Chem. 36 (4) (2012) 891–902.
[55] A.O. Eseola, W. Li, W.-H. Sun, M. Zhang, L. Xiao, J.A.O. Woods, Dyes Pigments 88 (2011) 262–273.
[56] A.O. Eseola, M. Zhang, J.-F. Xiang, W. Zuo, Y. Li, J.A.O. Woods, W.-H. Sun, Inorg. Chim. Acta 363 (2010) 1970–1978.
[57] G.M. Sheldrick, Acta Crystallogr. A A64 (2008) 112–122.
[58] A. Albert, E.P. Serjeant, The Determination of Ionization Constants, Chapman and Hall, USA, 1984, pp. 70–101.
[59] A.O. Eseola, D. Geibig, H. Görls, W.-H. Sun, X. Hao, J.A.O. Woods, W. Plass, J. Organomet. Chem. 754 (2014) 39–50.